Finite Element Optimisation of a Shift Fork for Racing Applications

U1514864 May 2, 2019

Summary

This report details the optimisation of a transmission shift fork for automotive racing applications. A preliminary form was modified to reduce weight whilst constrained by specified criteria for stress and deflection. Linear and non-linear finite element analyses were conducted to verify these criteria. This process was iterated towards an optimised design where a linear analysis was conducted to determine the part's dynamic characteristics. The final version was made of a PEEK/Carbon composite and, along a unique truss structure, attained total weight savings of 1.17 kg or 91 %, with full compliance of the design specification. The proposed design consists of complex geometry yet is well suited to injection moulding, overmoulding or additive manufacturing techniques. It is highly fatigue resistant and well suited to demanding applications in competitive motor-sports.

1 Introduction

1.1 Practical application of a shift fork

A shift fork is a key component that underpins the operation of modern manual transmissions. These are ubiquitously synchronised; most gear pairs are meshed constantly. For a particular pair to be selected, a synchroniser locks the chosen gear to the rotation of the drive shaft through friction. The shift fork enables this by actuating a sleeve that joins the gear, synchroniser and the hub on the drive shaft, thereby matching their velocities.

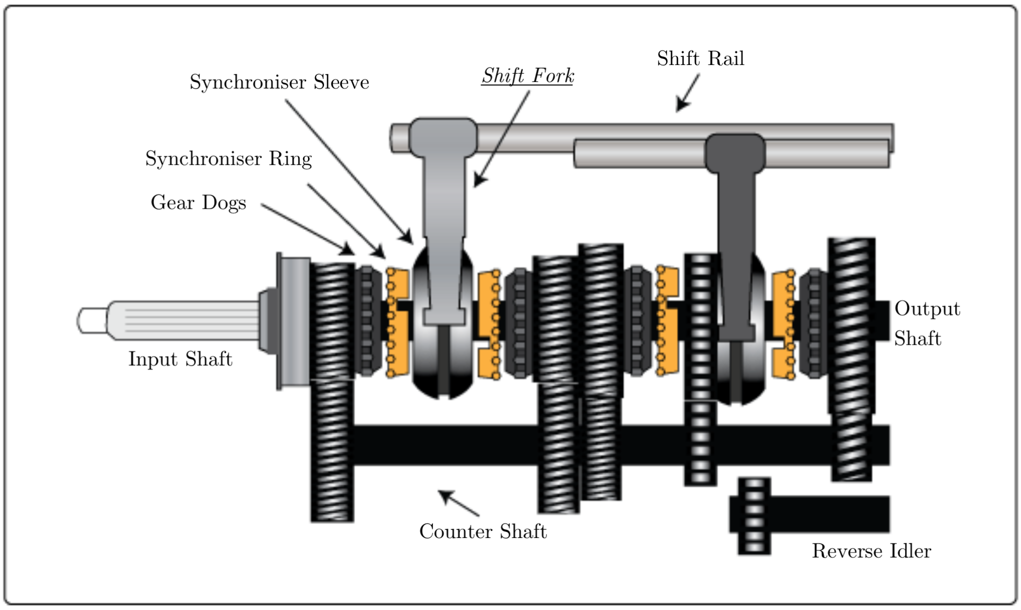

Figure 1: Annotated synchromesh transmission

1.2 FEM theory

The Finite Element Method is a versatile analytical tool; it refers to the discretisation of a physical model into individual elements. The matrix stiffness equations are evaluated for each element and then combined to approximate the whole structure via numerical solutions to their structural partial differential equations. Each element is a simple geometric shape connecting distinct nodes that make up the structure. The 'mesh' is the network used to describe the collection of elements and nodes in a structure. Refinement of the mesh requires an increased count of nodes and therefore elements, increasing the accuracy and resolution of analysis - at the cost of time and computational power.

1.3 Introduction and overall approach

The aim of this report is to provide an optimised design for a shift fork through a process of iterative improvement starting from an initially specified design. Each further iteration was justified by the results of finite element tests, conducted using Abaqus CAE software. Each iteration was developed as a model in SolidWorks through modifications to geometry, including extruded and revolved cuts. Further changes were made to optimise the material, aided by Granta's CES Edupack material selection software.

1.4 Specification and aims of the analysis:

To ensure the final design retained the core function of a shift fork certain dimensions were fixed and a minimum criteria for stress and deflection was specified. The loading instances varied by the nature of the analysis; in the static linear tests - this was via a distributed pressure without contact considerations (acting on the fork only). In the non-linear analyses the load was imparted as a concentrated force on an assembly of the fork and a representation of a synchroniser sleeve. This accounted for the contact between both components. The design criteria for stress and deflection are given below:

- Maximum allowable (axial) shift fork deflection = 0.20 mm
- Maximum allowable peak stress < yield strength of chosen material

2 Model generation

2.1 Form and geometry

According to the prescribed initial design, the part was sketched and constructed via SolidWorks. The shape was extruded, and an offset cut made to form the recessed section which engages the sleeve. This was transferred into Abaqus using the IGES (Initial Graphics Exchange Specification) format. This process was repeated for each design iteration and the edges merged to resolve incompatibilities as each part was converted to an analytical representation. In the non-linear analyses, the sleeve was represented by an analytically rigid disk of 48 mm diameter. This was then rotated and translated into a position of contact with the internal lip of the shift fork.

2.2 Partitions & mesh structure

A series of partitions were imparted onto the model, dividing it into distinct segments. These allow a mesh to be better distributed over irregular geometries producing a uniform mesh density. Hexahedral elements were used throughout for their improved accuracy and computational efficiency (Mottram, 1996). Figures 3 (a-f) show this mesh restructuring with further changes detailed throughout the rest of this report, where appropriate.

3 Linear analysis of the initial design

For a preliminary linear analysis, the load was implemented as an equivalent pressure of 1.825 MPa acting over the contact lip. This was calculated by dividing the force of 1055 N over the lip area (a semi-annulus where r_o = 48 mm and r_i = 44 mm):

$$P = \frac{F}{A} = 1.825 \text{ MPa} \quad \text{where} \quad A = \frac{\pi}{2}({r_o}^2 - {r_i}^2) = 578 \text{ mm}^2 \tag{1}$$

The only boundary condition was an encastre fixing of the inner surface of the hole at the top of the fork. This allows connection to the shift rod and ultimately, the shift lever.

3.1 Linear analysis of the initial design

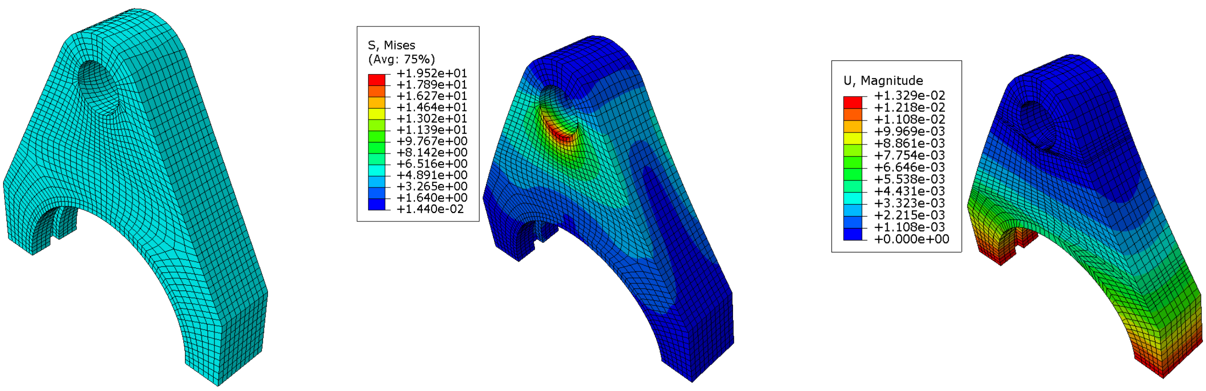

(a) Meshed part (b) Isometric stress plot (c) Isometric displacement plot

Figure 2: Visualised results: linear analysis of initial part

3.1.1 Evaluation

These plots depict the results of this analysis using a seed size of 2.5 mm and the mesh shown in Figure 3 (a). The peak stress was found to be 19.5 MPa and the greatest deflection was 0.03 mm confirming that the design can be optimised much further within the specification. The results give a sense for the area and magnitude of the deflections and stresses, allowing for mesh refinement. Further partitions were then imparted at the highest average concentrations of stress and displacement at the rail hole and prong ends; these are displayed throughout Figures 3 (a-f). The mesh was also tightened to reduce element distortion using an eventual global seed size of 2 mm.

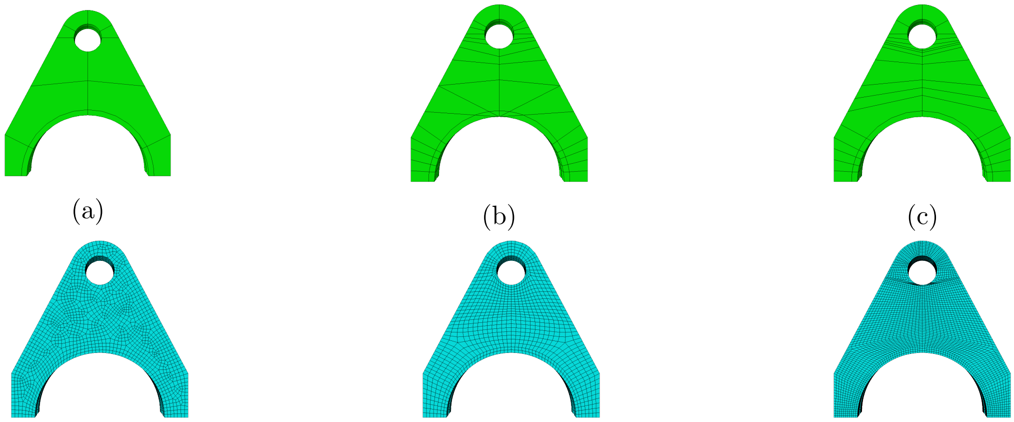

(a) (b) (c)

(d) (e) (f)

Figure 3: Selective refinement of partitions and mesh structure

4 Non-linear analysis of the initial design

A shift fork is loaded through its interactions with the synchroniser sleeve. A linear analysis is therefore insufficient in simulating the highly non-linear nature of the contact between both components, as well as the non-linearities arising from geometrical and material deformation. The following analyses simulate the effect of loading, whilst also accounting for the contact between the fork and the synchroniser sleeve.

The sleeve was modelled as a rigid disk (the master surface) and instanced into an assembly with the fork, as shown in Figure 4. The load was simulated as a concentrated force of 1055 N acting at the midpoint of the disk. The disk was constrained to displace axially only, in the z - plane, or along the axis defined by its midpoint. The interaction was specified as normal mechanical behaviour with hard contact and then constrained with finite sliding as defined by the Abaqus interaction module.

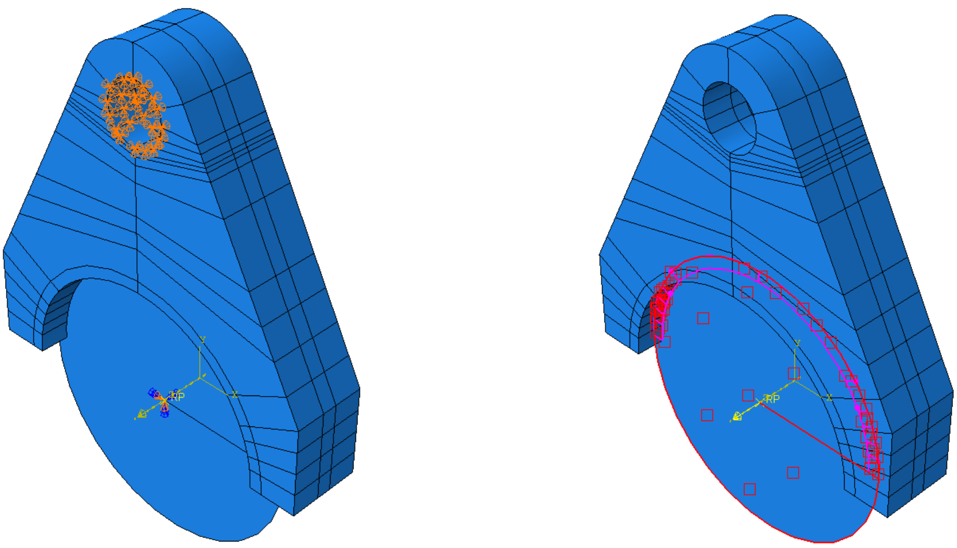

(a) (b)

Figure 4: Non-linear assembly showing a) boundary conditions and b) contact interaction

4.1 Results: non-linear analysis of initial design

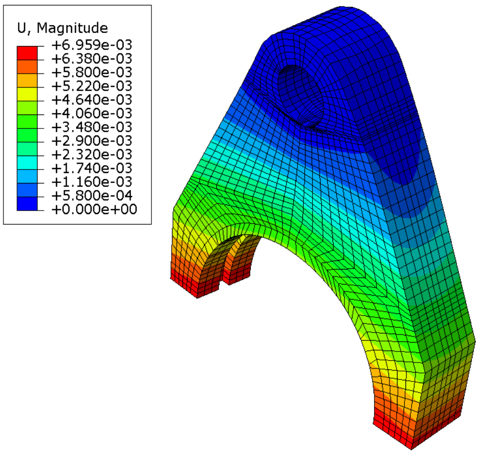

(a) Isometric plot - displacement

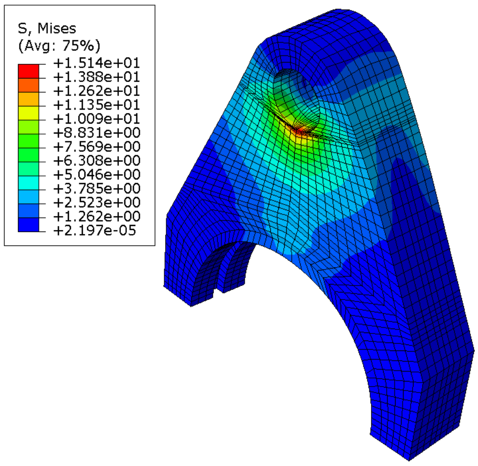

(b) Isometric plot - stress

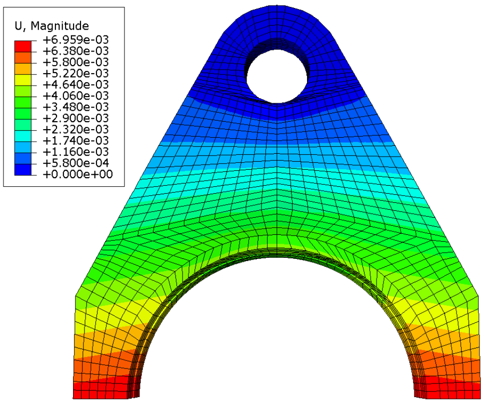

(c) Front plot - displacement

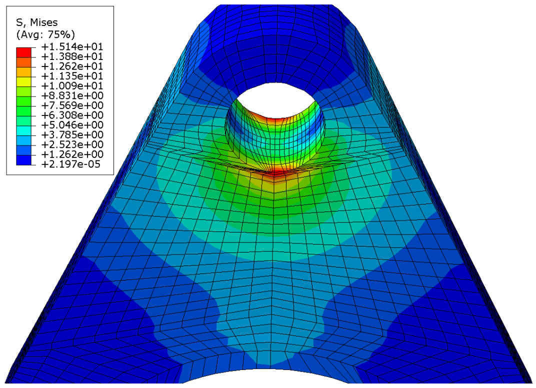

(d) Front plot - stress

Figure 5: Visualised results: non linear analysis of initial part

4.2 Evaluation

Compared to the linear results, differences are apparent in the stress plots of Figure 5. The biggest stress concentrations, towards the bottom of the rail hole, are narrower vertically (Figure 5d) and the overall stress distribution is narrower horizontally (Figure 5b). The stresses in the linear analysis reach further into the fork's prongs whereas here they are confined closer towards the middle. This could suggest that more material may be removed from the prongs, as the nonlinear analyses are more representative of real use.

The magnitude of the stresses and deflections lie at 15 MPa and 0.007 mm respectively. Considering the yield strength of mild steel (250 MPa) and the maximum allowable deflection (0.2 mm), the respective proportions are 6 % and 3 % of the design limits. Using the query feature and the density of mild steel at 7.8 $\times 10^{-9}$ tons per mm^3, the mass of the part was found to be 0.00128 tons or 1.28 kg. The following iterations attempt to reduce this, as much as possible, via modifications to the material and geometry. The above plots and peak values show that there is considerable scope for optimisation.

5 Design iteration (1) : material selection

The first design stage attempts to change the part material only. In working towards an optimised design, this was required in advance of changes to geometry as material properties exist in finite, discrete sets. If geometry optimisation was conducted first, it would not be guaranteed that an exact material would have properties that satisfy this geometry at the desired stress and deflection criteria; a compromise would have to be made when choosing between materials. This problem is eliminated by prior selection of the material.

Material selection was conducted using Granta Design's CES Edupack software. This is a material database that allows comparison of engineering materials using numerical constraints for specific material properties. A filter was imposed to select materials with a specific ratio of yield strength to density greater than 0.2 (MPa : Kgm^{-3}). Another filter eliminated any material with a Young modulus of less than 50 GPa. The following four materials were then chosen for further consideration as an optimal material.

Table 1: Shift fork material choices

Material	**Young Modulus (GPa)**	**Yield Strength (MPa)**	**Density (Kgm^{-3})**	**Fatigue Strength at 10^7 cycles (MPa)**
Mild Steel	210	250	7800	335
Aluminium 7075 (T6) alloy	68	552	2350	162
Titanium $\alpha - \beta$ alloy	119	1170	4505	630
Beryllium I-250	303	528	1850	207
PEEK/Carbon composite	148	2420	1560	1400

5.1 Conclusion and result

Each of these four materials offers an improvement over steel in one way or another though they have been considered by their mechanical properties only at this stage. Further consideration is given to the cost and manufacturing implications later in Section 9. The PEEK composite polymer was determined to be the optimum choice as its strength : weight ratio is 5x that of the second highest in this metric (Beryllium).

The reduced stiffness of PEEK may result in greater displacements however, its massively reduced weight was considered to be worth the compromise (it is 5x less dense than steel but only 0.7x the stiffness). Furthermore, the PEEK/Carbon composite is a proven high-end automotive material which has previously been used for racing shift-forks (Victrex, 2017). For the initial part model, the use of PEEK results in a mass of 0.256 kg - a saving of 1.024 kg or an 80 % decrease through material selection alone.

6 Design iteration (2) : I-beam profile

This iteration imposed changes to the part geometry using an extruded cut (mirrored about the mid-plane) throughout the inner volume. This left a thin 'web' profile of 5 mm thickness. This web provided structural support whilst the outer 5 mm of the profile were unchanged to maintain some rigidity. This effectively created an I-beam cross section. The immediate 5 mm surrounding the rail hole and the prong-ends were unchanged to maintain even contact and operation. Compared to the initial design made of PEEK (iteration 1), the decrease in weight is 44 %, down to 0.143 kg.

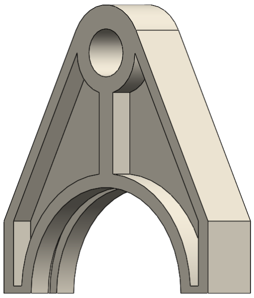

Figure 6: Second iteration part model

6.1 Analysis and results

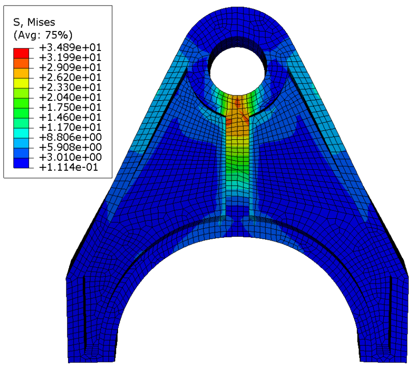

(a) Front plot - stress

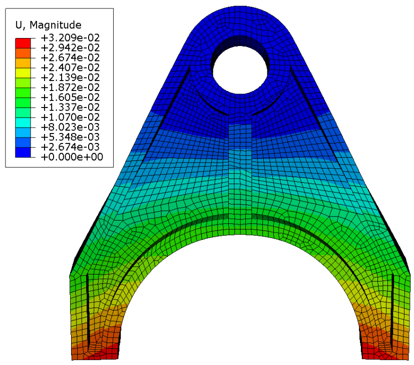

(b) Front plot- displacement

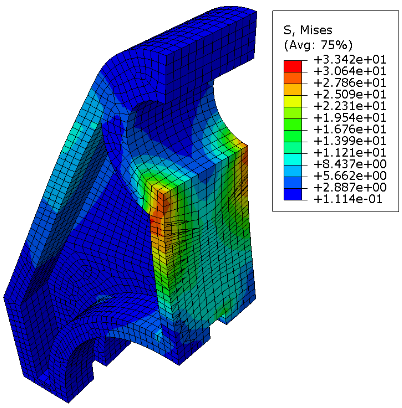

(c) Y plane cut - stresses

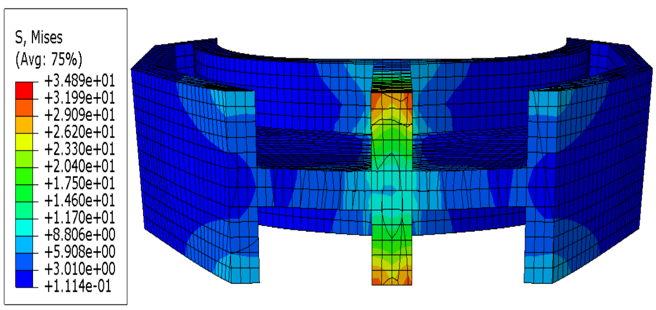

(d) X plane cut - peak stresses

Figure 7: Visualised results: analysis of second iteration

6.2 Evaluation

This iteration presents higher peak stresses; 35 MPa compared to 15 MPa for the initial design. This is still well under the yield and fatigue limits (1.4 - 2.5 %). The stresses are less concentrated but consistently higher as a fraction of the peak value. The peak deflections are much higher; 0.032 mm where before they were 0.007 mm. It is suggested that the central member be redesigned to reduce the stress concentrations further.

7 Design iteration (3): truss structure

This third iteration modifies the previous one by reducing the entire part thickness by 5 mm. The rib was replaced by a truss structure consisting of 3 mm thick members. Material was also removed from the contact lip to leave only the prong ends as contact surfaces. This allowed the removal of material to a radius of 55 mm for further weight reduction. This combination resulted in a new weight of 0.109 kg representing a further saving of 34 g or a percentage decrease of 24 %.

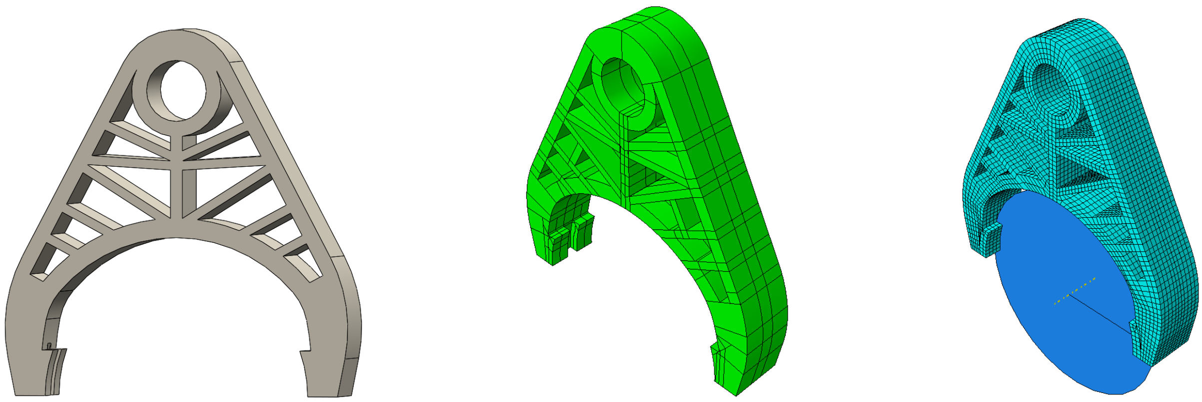

(a) (b) (c)

Figure 8: Third iteration part model, partitions and mesh structure

7.1 Analysis and results - plots overleaf

7.2 Evaluation

The plots in Figure 9 depict the results of non-linear analysis of the third iteration. The changes to the design can be seen to effectively reduce the stress concentrations formerly present between the rail hole and the central member. The peak stress occurs at the contact interface with a magnitude of 178 MPa and the corresponding contact pressure is 1197 MPa. The former is well under the yield strength of the PEEK/Carbon composite at 2420 MPa; the relative proportions is 7 % . Though the contact pressure can be neglected structurally, it is still under the yield and fatigue limits. The fatigue strength of the PEEK composite is 1400 MPa meaning that fatigue failure is extremely unlikely unless thermal effects become significant. The displacement peaked at 0.19 mm axially, relative to the rail connection. This was the limiting factor in the optimisation process - being 96 % of the design criteria.

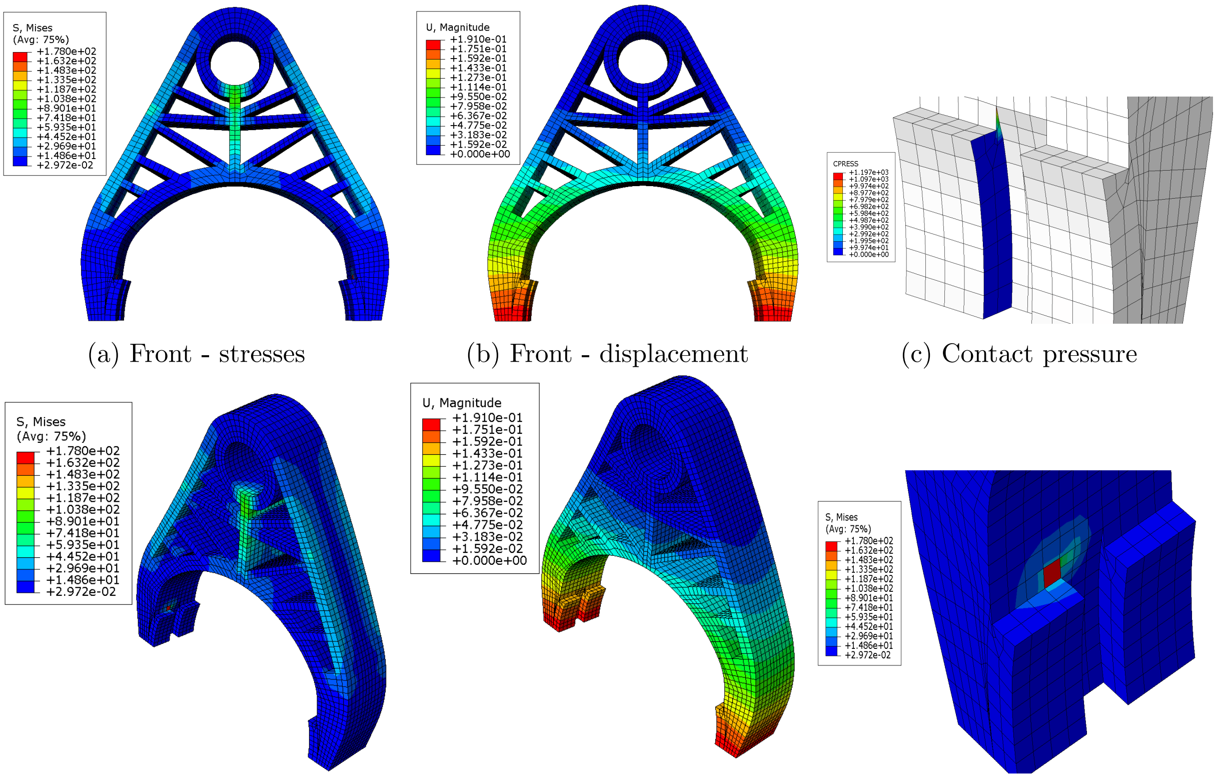

(a) Front - stresses (b) Front - displacement (c) Contact pressure

(d) Isometric - stresses (e) Isometric - displacement (f) Closeup - peak stress

Figure 9: Visualised results: analysis of third iteration

7.2.1 Evaluation of methodology, mesh refinement and convergence

The above results were obtained with a structured mesh at a global seed size of 2 mm. It is important to realise that these results vary with the level of mesh refinement. This section attempts to address these variations to determine the critical mesh density for efficient computation. The analyses of the final design were repeated for different global seed sizes from 10 mm down to 1.2 mm. It was not feasible to test seed sizes lower than this with the available hardware.

It is clear from Figure 10 and Table 2, overleaf, that the use of a seed size of less than 4 mm produces drastically different results than at larger levels. A seed size of 2 mm was deemed to be an appropriate compromise between accuracy and computational efficiency so the final non-linear results were taken at this level. The displacement results are seen to converge sooner than the stresses at an estimated seed size of $\sim$ 1 mm, as is typical (Kim, 2014). Further tests will be necessary to precisely determine the true extent of mesh convergence for this geometry although the 4 mm seed size was shown to be a significant turning point.

Table 2: Comparison of analysis results and mesh refinement

— Seed size (mm)	Number of elements	Computation time (s)	U_{max} (mm)	S_{max} (MPa)
10	1176	21	0.2100	99.8
9	1254	20	0.2060	99.79
8	1278	20	0.2005	98.51
7	1416	20	0.2008	99.21
5	1790	20	0.2043	100.2
4	2070	20	0.2038	100.9
3	4292	26	0.1981	101.3
2.25	7472	33	0.1945	173.6
1.75	17964	68	0.1867	201.3
1.6	19823	104	0.1869	200.5
1.2	49352	247	0.1844	393.5

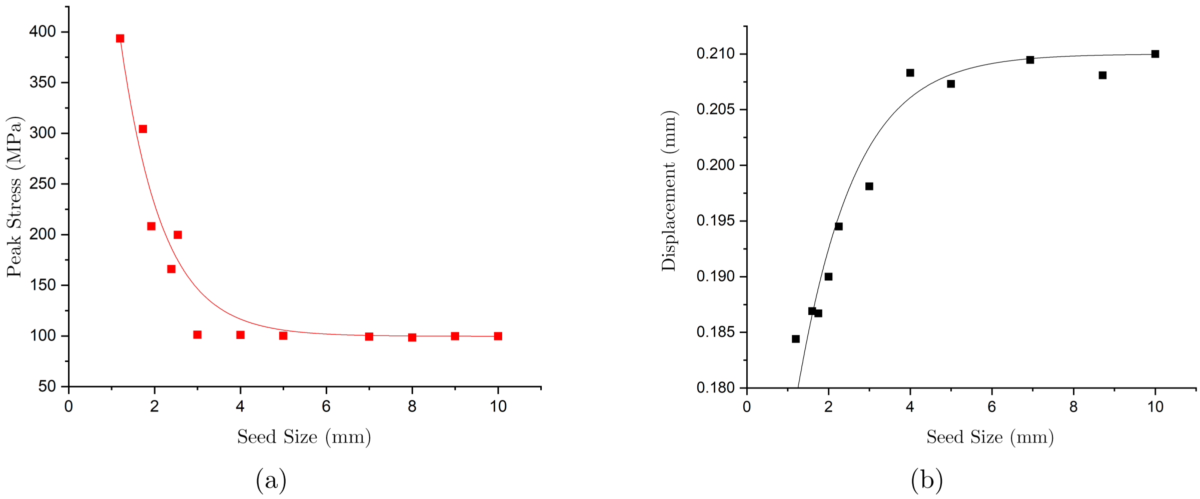

Figure 10: Plots of peak stress (a) and displacement (b) against global seed size

7.3 Linear dynamic analysis

It is important to approximate the fork's dynamic characteristics and modes of vibration to prevent sudden failure from resonant excitation. An dynamic model was used to approximate the natural (resonant) frequency of the fork using a linear perturbation step. This was found by comparison to the effective mass component at each mode of vibration. The natural frequency corresponded to the second mode with an effective mass of 91 g. This was closest to the total effective mass in the Z - plane at 65 g and thus was the most effective mode; the corresponding frequency was 2257 Hz. This is enough to determine that failure is unlikely via resonance - as the transmission would need to be shifted 2257 times per second. However, it remains to be seen if high-frequency vibrations from other engine or transmission components could propagate to the shift fork and excite this mode. As such, it will be necessary to conduct a Systems Integration Test (SIT) when installed in a vehicle - to determine whether external vibrations can interfere with the fork.

7.4 Validation from first principles

The following subsection will attempt to verify whether the analyses were conducted appropriately by comparing their results to those obtained from first principles: both statically and dynamically. These calculations were performed with classical elastic theory and are limited in their accuracy with complex 3D structures. Rather, they were used to verify the general FEM approach and ensure a correct order of magnitude.

7.4.1 Static characteristics

A basic verification of the results was performed by modelling the shift fork as a cantilever with the prongs considered to be structural members. Equations 2 to 4 show the employed formula from the engineering databook; E is the young modulus (148 GPa), L the member length ($\sim$ 80 mm) - taken to be the straight outside edge of the main diagonal members, y the member height (5 mm) and W the external load (1055 N). The moment of area I of the shift fork members about the z-plane was found, using the section-properties evaluation feature in SolidWorks, to be $\sim 4 \times 10^{-9}$ m^4.

$$\text{Displacement of an end-loaded beam:} \quad y_{max} = \frac{WL^3}{3EI} = 0.27 \text{ mm} \tag{2}$$

$$\text{Peak bending stress:} \quad \sigma_{max} = \frac{My}{I} = 106 \text{ MPa} \tag{3}$$

These values differ considerably from the numerical results with percentage differences of up to 40 %. Some justification is provided by the extent of the differences between classical mechanics and the finite element method. The orders of magnitude are the same as those computed, so it can be assumed that the FEA methodology was sufficient.

7.4.2 Dynamic characteristics

For dynamic validation, the part was modelled as a simple harmonic oscillator and the natural frequency found with the mass of 109 g and displacement, as calculated above:

$$f = \frac{1}{2\pi}\sqrt{\frac{k}{m}} = 952 \text{ Hz} \qquad \text{Where } k = \frac{W}{y_{max}} = 3.9 \times 10^6 \text{ Nm}^{-1} \tag{4}$$

This predicted natural frequency is less than half that found from the linear perturbation step which highlighted the top twenty modes of vibration. The lowest of these was 1930 Hz and the resonant frequency was 2257 Hz. This discrepancy is high though feasible given the complexity of the part stiffness compared to a simple mass-spring system. Practical dynamic testing is recommended to thoroughly evaluate these differences.

8 Final design - technical drawing

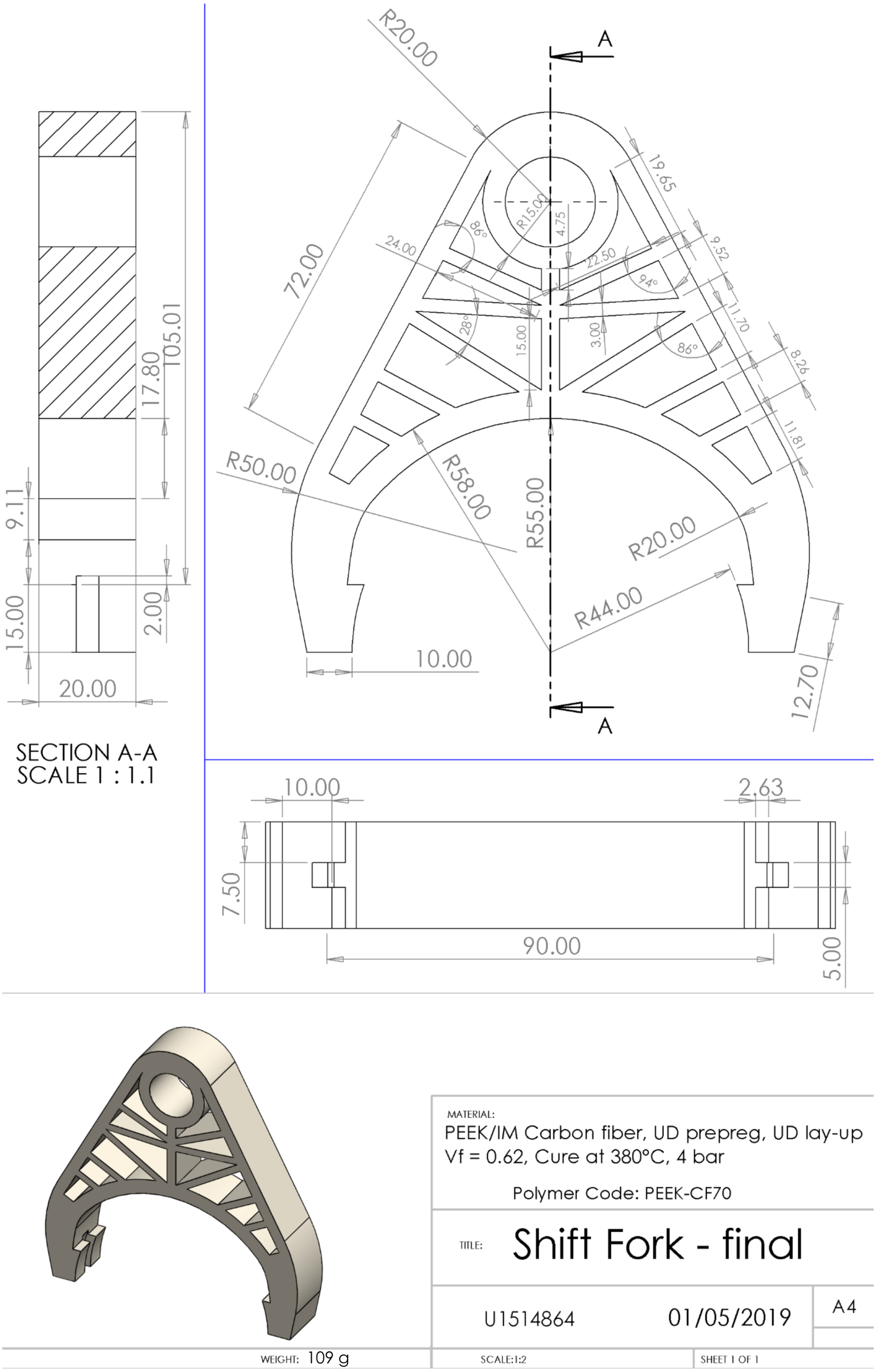

8.1 Implications for cost and manufacture

The final design specifies the use of a PEEK/Carbon composite polymer with a unidirectional, pre-impregnated structure. The geometry is complex and would normally require extensive CNC milling however, PEEK can be formed through injection moulding and overmoulding processes (Victrex, 2017). The part is therefore suitable for quick, high-volume production.

PEEK is approximately 60 % more expensive per unit volume than a similar titanium alloy. The density of the PEEK composite is just 35 % that of titanium so its use is economical if the weight saving is the ultimate aim. It can be formed into the required geometry with minimal tool wear compared to harder metals. The part will be costly in low volumes given the expense of the material but demand should exist beyond racing, as there is an inevitable trend towards stricter emissions control. This demands lightweighting across all vehicle types so high volume, economical production is likely still.

9 Conclusion

This report has demonstrated the use of FEA to effectively optimise a transmission shift fork. Non-linear analyses were conducted to ensure the final design met its criteria for stress and deflection. The results of 178 MPa and 0.19 mm, respectively, proved the part's integrity and fatigue resistance. A linear dynamic analysis was also conducted to determine the natural frequency at 2257 Hz. All this was accomplished with an overall weight saving of 1.17 kg. This was achieved via the use of an advanced PEEK/Carbon composite as well as a unique truss structure. Ultimately, the design is a substantial improvement and is well suited to high-performance automotive racing applications.

10 Recommendations for further work

The following actions would further the development of the shift fork and improve upon the work of this project:

- Repeated analyses with tighter mesh densities (seed sizes < 1 mm) using faster, multi-core CPUs and more memory or, alternatively, with a server cluster set-up
- Repeated analyses with more realistic assembly instances and contact interactions eg. inclusion of the shift rail and/or synchroniser ring
- Comparison of the final design to one produced with a numerical optimisation process (using generative design or topology optimisation software)
- Conduct thermal FEA and CFD analyses to determine changes to mechanical behaviour under the increased operating temperatures of a gearbox
- Construction of a physical prototype for the following:
  - Conduct practical modal analysis tests using a load cell or EM transducer
  - Test for corrosion and chemical interactions with intended lubricants

Bibliography

Fischer, R. (2015). *The Automotive Transmission Book*, Powertrain, Springer International Publishing.

Kim, N. (2014). *Introduction to Nonlinear Finite Element Analysis*, Springer US.

Kunal, R. (2011). *Gear Shift Fork Stiffness Optimisation*, SAE Technical Paper Series [2011-01-2235] .

Liu, Z. S., Zhang, X. H. and Gao, X. Q. (2013). *Topology Optimization of the Transmission Shift Fork*, Applied Mechanics and Materials **325-326**: 167171.

Mottram, J. T. and Shaw, C. T. (1996). *Using Finite Elements in Mechanical Design*, McGraw-Hill.

Okereke, M. and Keates, S. (2018). *Finite Element Applications: A Practical Guide to the FEM Process*, Springer Tracts in Mechanical Engineering, Springer International.

Victrex-PLC (2017). *Victrex Polymer Solutions: Driving Innovation in Powertrain Applications*, [PDF] Victrex Powertrain Solutions.

Yildiz, A. R., Kaya, N., Ozturk, F. and Alankus, O. (2004). *Design of Vehicle Components using Topology Design and Optimisation*, International Journal of Vehicle Design **34**(4): 387.

Zhang, Y. and Mi, C. (2018). *Automotive Power Transmission Systems*, Automotive Series, Wiley.